Journal of Colloid and Interface Science 368 (2012) 462–469

Contents lists available at SciVerse ScienceDirect

Journal of Colloid and Interface Science

www.elsevier.com/locate/jcis

Vanadium oxide intercalated with polyelectrolytes: Novel layered hybrids with anion exchange properties

Fernando J. Quites [a], Chiara Bisio [b], Rita de Cássia G. Vinhas [c], Richard Landers [c], Leonardo Marchese [b], Heloise O. Pastore [a,*]

[a] Institute of Chemistry, University of Campinas, R. Monteiro Lobato, 270, Cidade Universitária Zeferino Vaz, 13084-971 Campinas, SP, Brazil
[b] Dipartimento di Scienze e Tecnologie Avanzate, Universitá del Piemonte Orientale, Viale Teresa Michel, 11, 15100 Alessandria, Italy
[c] Applied Physics Department, Gleb Wataghin Physics Institute, University of Campinas, 13083-970 Campinas, SP, Brazil

ARTICLE INFO

Article history:
Received 9 August 2011
Accepted 7 November 2011
Available online 16 November 2011

Keywords:
Vanadium oxide
Polyelectrolytes
Intercalation reactions
Redox reactions
Cyanine dyes
PDDACl
PAHCl
Anionic exchanger

ABSTRACT

Novel anion exchange hybrid materials were developed by the insertion of poly(diallymethylammonium chloride) (PDDACl) and poly(allylamine hydrochloride) (PAHCl) polyelectrolytes into V_2O_5 interlayer spaces using hydrothermal treatment and were used to host an anionic cyanine dye. A systematic study of the hybrid material synthesis by direct *in situ* reaction of PDDACl and PAHCl polycations with V_2O_5 powders showed that the interlayer space of V_2O_5 expands from 0.44 nm to 1.40 nm and 1.80 nm upon intercalation of PDDACl and PAHCl polyelectrolytes, respectively. X-ray photoelectron spectroscopy and DR UV–Vis–NIR spectroscopy revealed that some V^{5+} sites were reduced to V^{4+} during the intercalation of the polyelectrolytes, these acted as both charge balancing entities for the negative oxide sheets and carriers for exchange sites located in the V_2O_5 interlayer space. The interlayer separation is consistent with the existence of coiled conformation of the polycations. The hybrid materials produced $[PDDACl]_{0.24}[PDDA]_{0.29}V_2O_5$ and $[PAHCl]_{0.28}[PAH]_{0.47}V_2O_5$, exhibited approximately 45.0% and 37.0% of chloride ions still available for anionic exchange, respectively. These materials were used to encapsulate a cyanine anionic dye. The presence of the dye was evidenced in the $[PDDACl]_{0.24}[PDDA]_{0.29}V_2O_5$ by significant fluorescence, with emission peak centered at 617 nm.

1. Introduction

Layered intercalation compounds have been receiving significant attention in recent years owing to their applications in various fields such as electrocatalysis [1], energy-storage applications [2], sensors [3], photochemical redox reactions [4], rechargeable batteries [5,6], heterogeneous catalysis [7] and ion exchange processes [8]. In particular, there is interest in the insertion of organic molecules and polymers into layered hosts for the purpose of synthesizing organic–inorganic composite materials with well-defined stoichiometries and organized structures [9].

Vanadium oxides, in particular vanadium pentoxide (V_2O_5), have attracted special interest because of the lamellar structure [10], the potential use as cathode materials for rechargeable lithium batteries and the important role in catalysis [4,7,11]. Its layered structure is constituted of parallel ribbons of VO_5 pyramids (Fig. 1) where the interlayer space can be used as an adequate space to host species to produce intercalation compounds. Some studies of such intercalation reactions involve hydrothermally prepared V_2O_5–alkylamines [12] and V_2O_5–pyridines [13] nanocomposites as well as V_2O_5–ethylenediamine [14], suggesting that lamellar vanadium pentoxide can be successfully employed as host material in intercalation reactions [15]. The studies performed by Murugan et al. [16,17] also showed that vanadium pentoxide is a good host for electrochemical intercalation of poly(3,4-ethylenedioxythiophene) for application in lithium batteries and supercapacitors. Therefore, intercalation reactions can convert a simple host into ordered inorganic–organic assemblies with structures controlled by host–guest and guest–guest interactions, leading to a rich variety of properties and applications [9].

With the exception of layered double hydroxides and hydroxyl double salts [19], almost all layered host materials, as well as many open framework hosts, present anionic frameworks, meaning that they can accept only cationic guests.

Taking these two aspects into consideration, ease of chemical modification in the interlayer space and the fact that the majority of layered materials are cationic exchangers, we investigated, in the first part of this work, the intercalation of poly(diallymethylammonium chloride) (PDDACl) (Fig. 2a) and poly(allylamine hydrochloride) (PAHCl) (Fig. 2b) polyelectrolytes into the vanadium pentoxide matrix, using only hydrothermal processes. The objective was to create ion exchange sites in the solid layers and, simultaneously, to produce a novel material with anionic exchange sites

* Corresponding author.
E-mail address: gpmmm@iqm.unicamp.br (H.O. Pastore).

0021-9797
doi:10.1016/j.jcis.2011.11.013

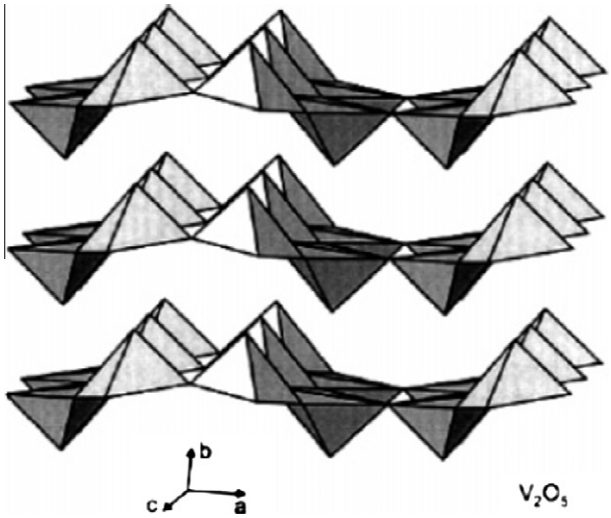

Fig. 1. Crystal structure of V_2O_5 consisting of layers of VO_5 square pyramids that share edges and corners. The apical V—O bond distance is much shorter than the four other distances and corresponds to a double bond [18].

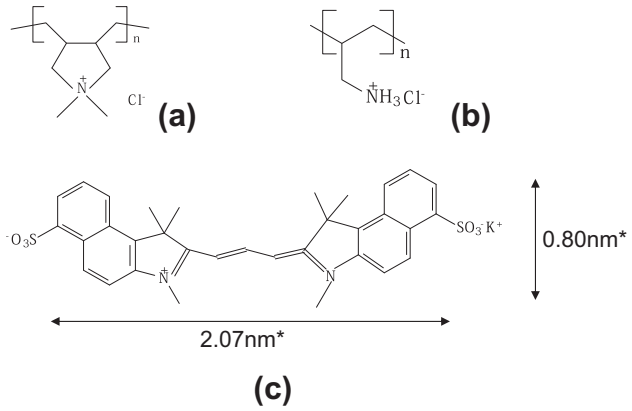

Fig. 2. Structure of the guest species studied: poly(diallyldimethylammonium chloride) (PDDACl) (a), poly(allylamine hydrochloride) (PAHCl) (b) and cyanine anionic dye (Iris 3.5-b) (c). *Sizes of dye calculated by DFT (B3LYP/cc-PVTz level).

into the V_2O_5 interlayer spaces by the occlusion of quaternary ammonium/chloride anions pairs, still capable of anion exchange.

In the second part of this study, we investigated the encapsulation of an anionic cyanine dye (Fig. 2c) by the [PDDA]–V_2O_5 hybrid produced. To incorporate large anionic guests, such as dye molecules, the chains of polycations should have the flexibility to coil on lower charge density layers, in this case polyelectrolytes are preferred, because of their ability to shield low charge density of layers [20]. This study shows that the hybrid materials produced here display large capacity as an anionic exchanger. The structure and the properties of these inorganic–organic intercalation compounds were revealed by a combined study based on powder X-ray diffraction (XRD), thermogravimetry (TG), Fourier-transformed infrared spectroscopy (FT-IR), scanning electron microscopy (SEM), diffuse reflectance ultraviolet–visible–near infrared spectroscopy (DR UV–Vis–NIR), X-ray photoelectron spectroscopy (XPS), ^{13}C CP–MAS NMR spectroscopy and fluorescence spectroscopy.

2. Experimental section

2.1. Materials

All reactants were used as received. Vanadium pentoxide (V_2O_5), the host material, was purchased from Merck, a 20.0 wt.% aqueous solution of high molecular weight (Mw 100,000–200,000) poly(diallymethylammonium chloride) polyelectrolyte (PDDACl) and powders of poly(allylamine hydrochloride) (PAHCl) Mw 15,000 were obtained from Sigma–Aldrich and the anionic cyanine dye (Iris 3.5b) was supplied by Cyanine Technologies (Turin, Italy). Deionized water was used throughout. It is important to comment that the pristine V_2O_5 used is free from V(IV) ions.

The intercalation of PDDACl and PAHCl polyelectrolytes in the interlayer spaces of vanadium pentoxide (V_2O_5), $[PDDACl]_y[PDDA]_xV_2O_5$ and $[PAHCl]_y[PAH]_xV_2O_5$, was performed as follows: V_2O_5 (1.65 mmol, Merck) was added to an aqueous solution of PDDA (16.5 mmol, Aldrich) or PAH (1.65 mmol, Aldrich) and stirred until a homogeneous suspension of the solid was obtained. The mixture was heated under hydrothermal conditions in a Teflon-lined stainless autoclave for 96 h at 150 °C. The green powders (indication of reduction from V^{5+} to V^{4+} ions) were filtered, washed with water and ethanol and air-dried at room temperature.

The intercalation of cyanine dye was carried out by the following method: a methanol solution of the anionic cyanine dye (0.52 μmol L^{-1}) was prepared and was added to 100 mg of $[PDDACl]_{0.24}[PDDA]_{0.29}V_2O_5$ hybrid material. The resulting suspension was vigorously stirred for 48 h at room temperature, followed by filtration and washing with copious amounts of methanol. After the exchange, Soxhlet extraction was performed using methanol as the solvent for 6 h. This step is very important to wash away dye molecules that do not interact with the hybrid material. The violet product obtained was dried at room temperature and, based in the results of CHN elemental analysis before and after the encapsulation of the dye, named $[PDDACy]_{0.08}[PDDACl]_{0.16}[PDDA]_{0.29}V_2O_5$. The same procedure was performed for the encapsulation of the anionic dye into $[PAHCl]_{0.28}[PAH]_{0.47}V_2O_5$.

2.2. Characterization

The obtained materials were characterized by X-ray diffraction (XDR) using a Shimadzu XRD7000 diffractometer (monochromated Cu Kα1, 40 mA, 30 kV) at room temperature over the range $1.5° \leqslant 2\theta \leqslant 50°$. Fourier-transformed infrared spectra (FT-IR) were recorded from 4000 to 400 cm^{-1} at 4 cm^{-1} resolution on a Nicolet 6700 spectrometer in pellets of samples dispersed in KBr at a concentration of 0.5 wt.%. Carbon, nitrogen and hydrogen analyses were performed in a Perkin-Elmer, model PE 2400, microelemental analyzer on solid samples. Solid-state nuclear magnetic resonance spectra for ^{13}C nucleus were obtained on Advance 400II$^+$ solid-state high-resolution spectrometer, with cross-polarization and magic angle spinning (CP–MAS), at a frequency of 100.64 MHz with an acquisition time of 50 ms and contact time of 4 ms, whose chemical shifts were referred to tetramethylsilane. Thermogravimetry and derivative thermogravimetry (TG/DTG) measurements were recorded on Thermal Analyses equipment model 5100-TA Instruments. Samples were heated from ambient temperature to 1000 °C at a heating rate of 10 °C/min under oxygen (50 ml min^{-1}). Diffuse reflectance UV–Vis–NIR spectra were measured with Perkin-Elmer Lambda spectrophotometer of powder samples dispersed in $BaSO_4$ at a concentration of 10.0 wt.%; the spectra were collected in the range of 200–1600 nm wavelength. X-ray photoemission spectra (XPS) measurements were carried with a VSW HA100 spectrometer using non-monochromatized Kα of Al (1486.6 eV). The data were obtained at room temperature, and typically the operating pressure in the analysis chamber was below 2×10^{-8} mbar. The calibration of binding energies (BEs) was performed with Au $4f_{7/2}$ core level at 8.4 eV, and BE of adventitious carbon (284.6 eV) was utilized for charging correction with all the samples. The error in all the BE values

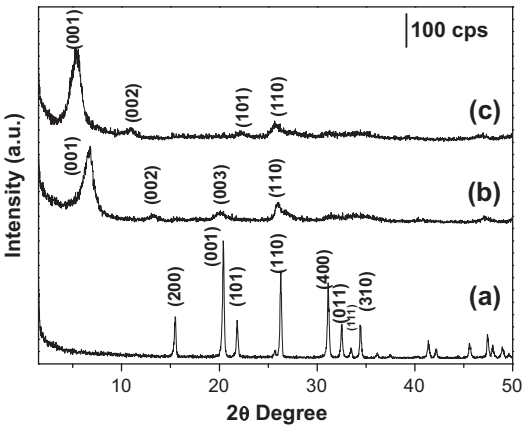

Fig. 3. Powder X-ray diffraction for the pristine vanadium pentoxide matrix (JCPDS 41-1426) (a), and for the $[PDDACl]_y[PDDA]_xV_2O_5$ (b) and $[PAHCl]_y[PAH]_xV_2O_5$ (c) hybrid materials.

reported here is within ±0.3 eV. Scanning electron microscopy (SEM) was performed in a Jeol 6360-LV, operating at 20 kV with the sample coated with carbon. Fluorescence spectra were collected by Horada Spectrofluorometer using Xe lamp with source excitation at room temperature.

In order to determine the amount of exchangeable chloride ions in the $[PDDACl]_y[PDDA]_xV_2O_5$ and $[PAHCl]_y[PAH]_xV_2O_5$, that is, the value of y in the formulas, Mohr's method was used [21]. Briefly, a solution of KNO_3 (5.2 mmol L^{-1}) was stirred with $[PDDACl]_y[PDDA]_xV_2O_5$ and $[PAHCl]_y[PAH]_xV_2O_5$ hybrid materials, and the supernatant was titrated with standard $AgNO_3$ (5.1 mmol L^{-1}) with the purpose to determine the quantities of exchangeable chloride ions.

3. Results and discussion

3.1. Structure and morphology of hybrids

V_2O_5 is a layered material formed of V_2O_5 ribbons and whose sheets are separated by a Van der Walls gap with a d-spacing of 0.44 nm [9,16]. Fig. 1 shows the structure of the oxide host before intercalation. V_2O_5 belongs to the orthorhombic system with *Pmmm* space group (JCPDS 41-1426). The insertion of PDDACl and PAHCl into the interlayer space of the oxide host causes important changes in the structure of the material. Fig. 3 shows the typical powder X-ray diffraction pattern for the vanadium pentoxide matrix (Fig. 3a) and for the intercalated compounds with PDDACl (Fig. 3b) and PAHCl polyelectrolytes (Fig. 3c).

The first difference to call attention on the XRD profiles is that polyelectrolytes intercalation cause the displacement of the (001) signal to low angles and the original interlayer space of V_2O_5 (0.44 nm) increases to 1.40 nm after reaction with PDDACl and to 1.80 nm upon intercalation with PAHCl. This large difference indicates that the PDDACl and PAHCl polycation chains within the interlayer space adopt a more coiled conformation in agreement with results obtained from Hata et al. [22]. This is not, however, the only difference. For the hybrid materials (Fig. 3b and c), the diffraction patterns present broad and low intensity peaks, suggesting a decrease in ordering with respect to the pristine matrix. The diffraction patterns showed here are also in good agreement with the results of XRD observed by Murugan et al. [16,17] for the intercalation of a conductor polymer into interlayer spacing of V_2O_5 oxide.

While producing a cationic layered host from vanadium pentoxide matrix, it is important to observe the morphology of the sheets (Fig. 4). From the SEM images of the vanadium pentoxide matrix (Fig. 4a), the presence the plates is observed while the hybrid materials show a more aggregated solid with still laminar features (Fig. 4b and c). More significantly, the incorporation of polyelectrolytes into V_2O_5 host is accompanied by morphological changes in agreement with the results of XRD patterns.

3.2. The guest

The guest species (PAHCl and PDDACl) were characterized by several techniques. The chemical formula of hybrids were calculated from results of elemental analysis, is summarized in Table 1 and was used to calculate the extent of organics intercalation. The content of anionic dye was calculated from the difference in carbon content before and after each reaction. The C/N ratio for the bulk PDDACl is 8.00 and for PAHCl is 3.00, while for the synthesized

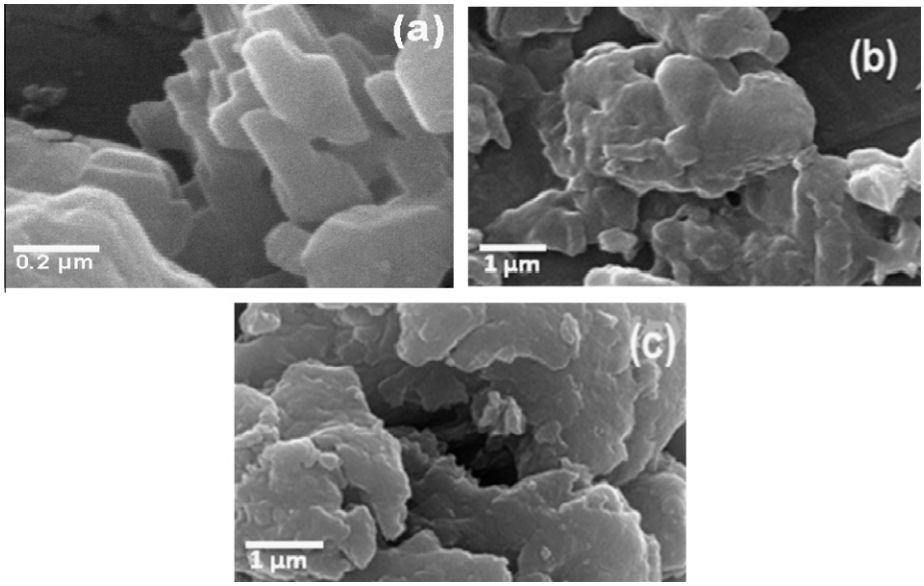

Fig. 4. Scanning electron micrographs of the vanadium pentoxide matrix (a), $[PDDACl]_{0.29}[PDDA]_{0.24}V_2O_5$ hybrid material (b) and $[PAHCl]_{0.28}[PAH]_{0.47}V_2O_5$ hybrid material (c).

Table 1
Unit cell chemical formula for the intercalation compounds.

Compounds	x	y	z[a]
$[PDDACl]_y[PDDA]_xV_2O_5$	0.29	0.24	–
$[PAHCl]_y[PAH]_xV_2O_5$	0.47	0.28	–
$[PDDACy]_z[PDDACl]_y[PDDA]_xV_2O_5$	0.29	0.16	0.08
$[PAHCy]_z[PAHCl]_y[PAH]_xV_2O_5$	0.47	0.20	0.04

[a] Calculated from the difference in carbon content before and after each exchange with dye.

hybrid materials, these ratios were 7.95 and 3.04, respectively, suggesting that the polyelectrolyte does not degrade upon the intercalation as was also verified by ^{13}C CP–MAS NMR spectra (Fig. 5, see below). The concentration of exchangeable Cl^- ions gives the percentage of ion exchange groups still available for reaction with anions and was calculated by the results obtained from Mohr's Method. Having in mind that the initial Cl/N in the pristine polyelectrolyte is one, after the reaction, there are, approximately, 45.0% of exchangeable Cl^- ions in the $[PDDACl]_{0.24}[PDDA]_{0.29}V_2O_5$ hybrid material and 37.0% of exchangeable Cl^- ions in the $[PAHCl]_{0.28}[PAH]_{0.47}V_2O_5$ hybrid material, in relation to the total cationic nitrogen atoms in the materials. Therefore, the capacity of anionic exchange in these materials was of 0.09 mmol of Cl^- exchangeable/100 mg of $[PDDACl]_{0.24}[PDDA]_{0.29}V_2O_5$ hybrid and 0.08 mmol of Cl^- exchangeable/100 mg of $[PAHCl]_{0.28}[PAH]_{0.47}V_2O_5$ hybrid. The results show that these compounds can be employed as anion exchangers. The larger quantity of sites available in the hybrid intercalated with PDDACl in comparison with the one prepared with PAHCl can be related to the pH of the intercalation reaction: as in PDDACl there is a quaternary ammonium site, changes in the pH of the aqueous reaction media do not modify the charge of the group. PAHCl on the contrary, depends on pH. Its pK_a in solution is approximately 8.7, and at the neutral pH of the intercalation, some amino groups are nonprotonated [23]. The presence of Cl^- ions was also observed by energy dispersion spectroscopy (EDS).

Solid-state high-resolution NMR spectroscopy was used to study the polyelectrolytes incorporated into the V_2O_5 structure. Fig. 5 shows the ^{13}C CP–MAS NMR spectra of PDDACl and PAHCl polyelectrolytes into the hybrid materials prepared in this work. The spectrum of PAHCl (Fig. 5A) showed broad peaks with chemical shift values of 31.5 and 44.0 ppm assigned to C—H and C—N groups of polymer units [23]. The ^{13}C CP–MAS NMR spectrum of the PDDA-based hybrid (Fig. 4B) showed peaks with chemical shifts of 70.8, 54.2, 38.9 and 27.3 ppm that are assigned to the CH_3 (a), CH_2 (b), CH (c) and CH_2 (d) groups in the PDDACl polycation [24]. The peaks of polyelectrolytes intercalated into hybrid materials are slightly displaced to higher chemical shift values in relation to ^{13}C CP–MAS NMR spectra of the free polyelectrolytes [23].

The thermal behavior of the hybrid materials was studied by TG/DTG under oxidizing atmosphere. The thermogravimetry and its derivatives for the V_2O_5 matrix and for the hybrids obtained in this work are shown in Fig. 6. For pristine vanadium pentoxide (Fig. 6a), the first mass loss is very small and appears in the region of 90 °C that is due to the exit of weakly bound water molecules. At much higher temperatures, there is a gain of mass (600 °C) which is associated with the oxidation of a small part of V^{4+} ions present in the V_2O_5 host, according to $2VO_2 + 1/2O_2 \rightarrow V_2O_5$ [25].

Fig. 6 b shows TG and DTG curves of $[PAHCl]_{0.28}[PAH]_{0.47}V_2O_5$, where four main mass losses are observed. The first one, in the range from 25 to 150 °C, is associated with the elimination of adsorbed water. It is followed by a mass loss between 150 and 260 °C, a third mass loss from 260 °C to around 360 °C and a last one in the range from 360 to 540 °C. The three last mass losses can be related mainly to the decomposition/oxidation of the PAHCl polyelectrolyte, indicating the presence of the organic polymer in vanadium pentoxide matrix. The $[PDDACl]_{0.24}[PDDA]_{0.29}V_2O_5$ hybrid material (Fig. 6c) also presents four main mass losses, as in the case of PAH hybrid, and is related with the elimination of water and the decomposition/oxidation of PDDACl polyelectrolyte.

The thermal stabilities of $[PDDACl]_{0.24}[PDDA]_{0.29}V_2O_5$ and $[PAHCl]_{0.28}[PAH]_{0.47}V_2O_5$ hybrid materials were also evaluated by calcining them at 600 °C for 3 h under O_2 (50 mL min^{-1}) atmosphere, at a heating rate of 10 °C min^{-1}. After the calcination, the obtained materials were cooled to room temperature and examinated by X-ray diffraction (XRD) and the FTIR spectroscopy.

Fig. 7 a shows the X-ray diffraction patterns, and Fig. 7b presents the FTIR spectrum of the calcined material. It can be observed that upon calcination all diffraction peaks of the orthorhombic V_2O_5 matrix are restored (Fig. 7a). For $[PAHCl]_{0.28}[PAH]_{0.47}V_2O_5$ sample, the same behavior was observed (not shown). The same effect was observed by FTIR spectroscopy (Fig. 7b): the typical vibrations of V_2O_5 lattice in the region from 1100 to 400 cm^{-1} are present in the spectrum of the calcined materials obtained either from $[PDDACl]_{0.24}[PDDA]_{0.29}V_2O_5$ or from $[PAHCl]_{0.28}[PAH]_{0.47}V_2O_5$ (not shown), indicating that the intercalation process does not alter the layered matrix.

3.3. Spectroscopic studies

Fig. 8 presents the FTIR spectrum of the vanadium pentoxide matrix (Fig. 8a) as well as the spectra of the intercalation compounds (Fig. 8b and c). The spectra of vanadium pentoxide (Fig. 8a) show the typical band at 1021 cm^{-1} assigned to the $\nu_{(V=O)}$, and at 837 cm^{-1} and 621 cm^{-1}, those are attributed to the in-plane (or symmetric) and out-of-plane (or antisymmetric) $\nu_{(V-O-V)}$ bending related to the V_2O_5 sheets [16,26].

The intercalation compounds (Fig. 8b and c) present bands slightly shifted in relation to the matrix, which may be caused by the interaction between the partially reduced vanadium ions in the vanadium pentoxide sheets and the polycation chains, leading

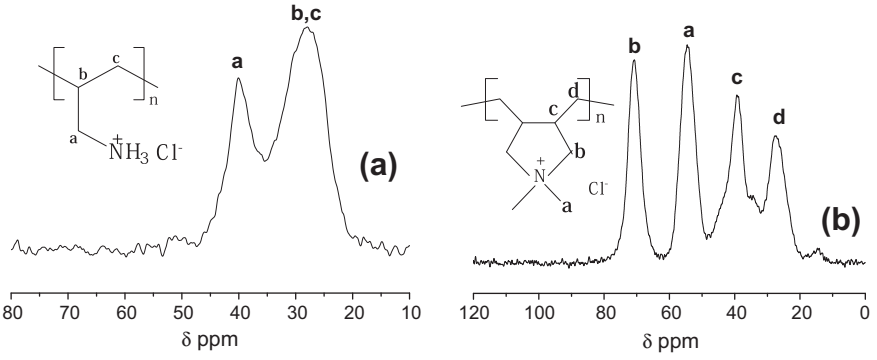

Fig. 5. ^{13}C CP–MAS NMR spectra of $[PAHCl]_{0.28}[PAH]_{0.47}V_2O_5$ (A) and $[PDDACl]_{0.24}[PDDA]_{0.29}V_2O_5$ (B) hybrid materials.

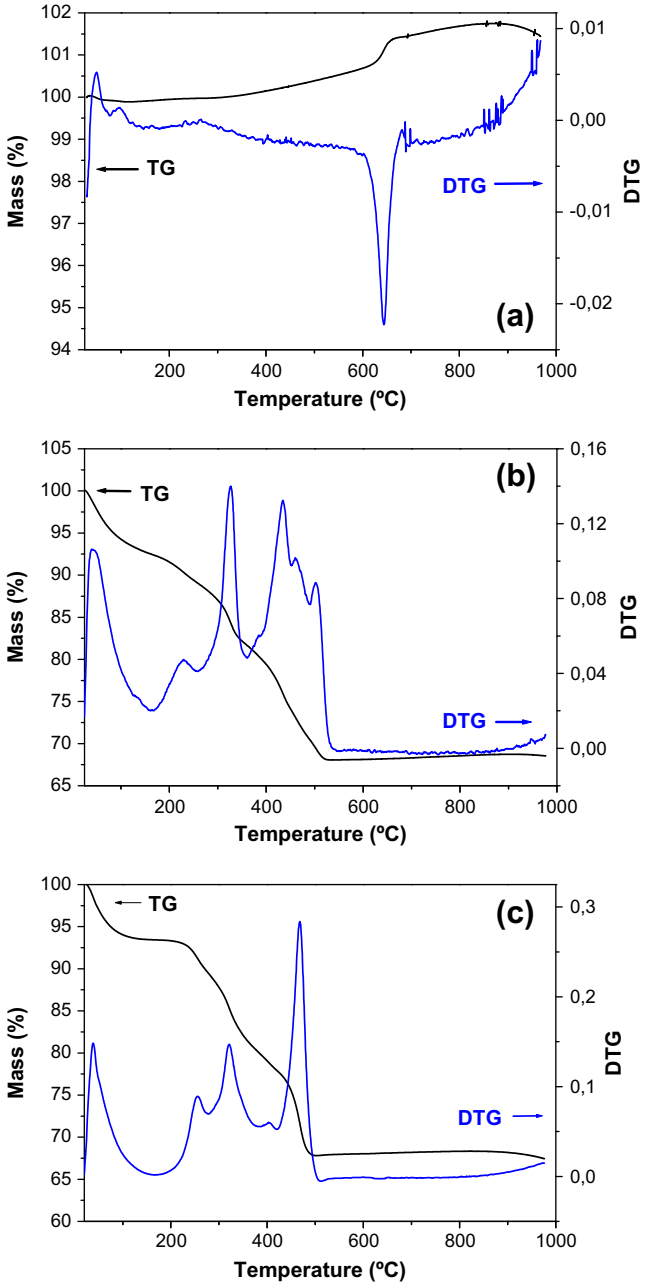

Fig. 6. Thermogravimetry analyses and their derivatives (TG/DTG) for the V_2O_5 matrix (a) and for the hybrid compounds $[PAHCl]_{0.28}[PAH]_{0.47}V_2O_5$ (b) and $[PDDACl]_{0.24}[PDDA]_{0.29}V_2O_5$ (c).

to weakened V=O bonds and V—O—V bonds [24]. In $[PDDACl]_{0.24}[PDDA]_{0.29}V_2O_5$ material, the peak assigned to the stretching vibration of V=O, $\nu_{(V=O)}$, appears at 1022 cm^{-1}, while for $[PAHCl]_{0.28}[PAH]_{0.47}V_2O_5$, it appears at 1006 cm^{-1}. The intercalation reaction also causes the appearance of a new band, at 987 $cm^{-1}$for $[PDDACl]_{0.24}[PDDA]_{0.29}V_2O_5$ and at 975 cm^{-1} for $[PAHCl]_{0.28}[PAH]_{0.47}V_2O_5$. These new bands can be associated with the V^{4+}=O stretching, $\nu_{(V4+=O)}$ [27,28]. Since V^{4+} ions have ionic radii larger than V^{5+} ions, the former would exhibit larger bond length, thus decreased vibration frequency. As the hybrid materials contain V^{4+} and V^{5+} centers, which have also been confirmed by UV–Vis–NIR and XPS spectroscopy (see below), the V—O—V vibrational absorptions shift from 852 cm^{-1} and 530 cm^{-1} to 758 cm^{-1} and 523 cm^{-1} [29]. In addition, the spectra of these new compounds (Fig. 8b and c) clearly show the presence of the characteristic vibration modes attributed to the organic phases: the sample with PDDACl polyelectrolyte shows bands at ca. 3015 (ν_{asym} of CH_3 groups bound to quaternary ammonium, not shown in the figure), 2927 and 2857 cm^{-1} (ν_{asym} and ν_{sym} of CH_2, not shown), 1465 cm^{-1} ($\delta_{(CH2)}$), and 3015 cm^{-1} ($\upsilon_{(CH)}$) (not shown). A band at 1600 cm^{-1} is also found along with a broad absorption at ca. 3440 cm^{-1} (not shown), which can be respectively assigned to bending and stretching vibrations of adsorbed water molecules .

The UV–Vis–NIR diffuse reflectance spectra of vanadium pentoxide matrix and of the hybrid materials produced from it are shown in the Fig. 9. It is interesting to observe that vanadium pentoxide matrix (Fig. 9a) displays a strong band around ca 260 nm that can be attributed to $\pi(t)2 \rightarrow d(e)$ oxygen to square-pyramidal V(V) charge-transfer transition [29,30]. A wide and strong absorption is observed in the range from 300 to 500 nm, which is composed of bands with many origins, such as $a_2(\pi)$, $b_1(\pi) \rightarrow b_2(xy)$ transitions owing to bridging oxygen in square-pyramidal coordination, $\pi \rightarrow \pi^*$ transitions and the charge transfer of the V=O double bond from oxygen to vanadium [31]. Absorptions similar to those discussed above were observed in the intercalation compounds (Fig. 9b and c). However, after polyelectrolytes intercalation, and as a consequence of the structural reorganization associated with the insertion of polycations, a new very broad absorption at 500–1600 nm is found, with a concomitant decrease in the intensity of the band at 300–500 nm (indicative of the reduction of V^{5+} sites) [32]. The presence of two oxidation states, V^{5+} and V^{4+}, with V^{4+} in a larger concentration in relation to V_2O_5, causes the increase of intensity for the intervalence bands in the NIR region, probably via polycation chloride oxidation. In conclusion, it is possible to propose that the chains of polycations are inserted within interlayer space of the matrix only upon a partial reduction of the oxidic layers and that they do so to counterbalance the charge generated in the oxide sheet. The mechanism of this remarkable interlamellar reaction is possibly coupled with the ability of vanadium centers to activate oxygen [29].

The hybrid materials were also measured by X-ray photoelectron spectroscopy (XPS). The core level XPS spectrum has been extensively used to characterize materials by the way of identification of the elements and their valence state and affords a semi-quantitative estimative of the relative amounts of the metal in the different valence states [5]. In this work, the samples were analyzed by XPS in order to identify the valence state of vanadium (V^{5+}/V^{4+}) after the intercalation of the polyelectrolytes.

Fig. 10a presents the XPS spectrum of V_2O_5. The spectrum of vanadium pentoxide shows two peaks located at 517.85 and 525.29 eV, which are due to the spin–orbit coupling V 2p levels $2p_{3/2}$ e $2p_{1/2}$, and they are related to absorption of V^{5+} ions only. Fig. 10b and c displayed the XPS spectra of V 2p and O 1s of $[PDDACl]_{0.24}[PDDA]_{0.29}V_2O_5$ and $[PAHCl]_{0.28}[PAH]_{0.47}V_2O_5$ hybrid materials after the removal of the O 1s X-ray satellite around 518–520 eV and after Shirley background subtraction. It is observed that the peaks of $V2p_{3/2}$ in the XPS spectra of the hybrid are broad and asymmetrical, which indicates that the vanadium atoms in these compounds are in different chemical environments. Deconvolution of the V 2p core levels clearly shows a low-BE feature at 515.41 eV assigned to $[PDDACl]_{0.24}[PDDA]_{0.29}V_2O_5$ and at 515.56 eV to $[PAHCl]_{0.28}[PAH]_{0.47}V_2O_5$, due to the absorption of V^{4+} ions. The above BE values are in good correspondence with the compounds reported in the literature [16,17,30]. Using the deconvoluted peak area of the V $2p_{3/2}$ level, the amount of V^{4+} is calculated to be 15% in the PDDA-based hybrid material and 21% for the hybrid based on PAHCl and V_2O_5 in relation to the total vanadium (V^{5+}). A similar trend was found in the DR UV–Vis–NIR spectra where the intervalence bands are more intense in PAH (Fig. 9c) than in PDDACl (Fig. 9b) intercalated materials. This clearly indicates a reduction of metallic oxide layers upon the

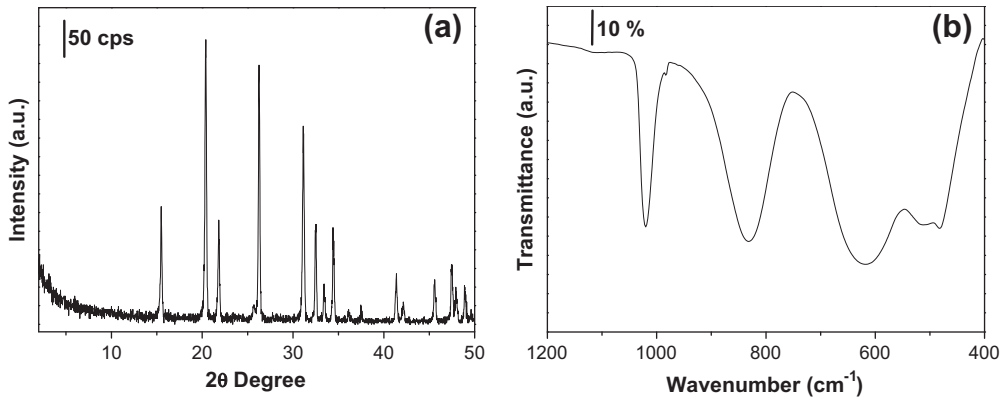

Fig. 7. Powder X-ray diffraction pattern (a) and FTIR spectrum (b) of $[PDDACl]_{0.24}[PDDA]_{0.29}V_2O_5$ hybrid calcined at 600 °C for 3 h in oxidant atmosphere.

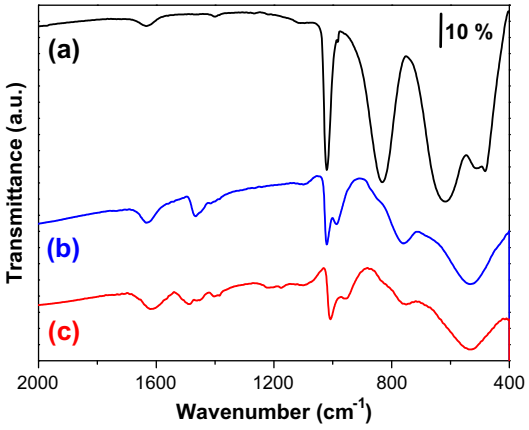

Fig. 8. FTIR of the vanadium pentoxide matrix (a), $[PDDACl]_{0.24}[PDDA]_{0.29}V_2O_5$ hybrid compound (b) and $[PAHCl]_{0.28}[PAH]_{0.47}V_2O_5$ hybrid compound (c).

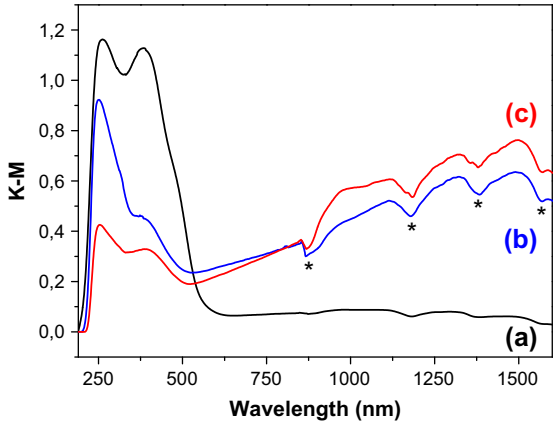

Fig. 9. UV–Vis diffuse reflectance spectra of pristine vanadium pentoxide (a) and $[PDDACl]_{0.24}[PDDA]_{0.29}V_2O_5$ (b) and $[PAHCl]_{0.28}[PAH]_{0.47}V_2O_5$ (c) hybrid materials. Asterisks indicate the intervalence bands.

intercalation of the polyelectrolytes, making it possible that an effective interaction between the polymer and V_2O_5 is established. Therefore, in accordance with the DR UV–Vis–NIR and FTIR spectroscopy, the intercalation of PDDACl and PAHCl into V_2O_5 interlayer spacing occurs when some V^{5+} are reduced to V^{4+} ions and a negative charge is created in the $V_2O_5^-$ layers where polycations are intercalated simultaneously bringing exchange sites to the interlayer space of the oxide.

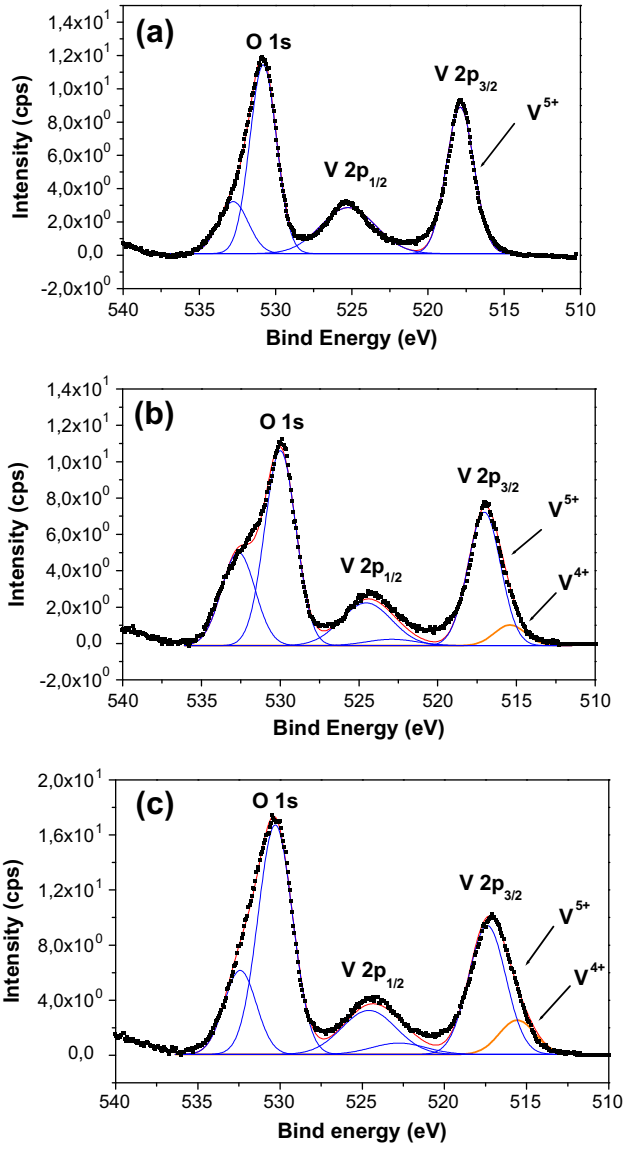

Fig. 10. X-ray photoelectron spectra of V 2p and O 1s levels of the V_2O_5 pristine (a) $[PDDACl]_{0.24}[PDDA]_{0.29}V_2O_5$ (b) and $[PAHCl]_{0.28}[PAH]_{0.47}V_2O_5$ (c) compounds.

The quantity of V^{4+} ions present in the hybrid materials as indicated by XPS spectroscopy can be correlated with the results found by elemental analyses (CHN) and by the Mohr's method. Through the formula obtained by carbon, nitrogen and hydrogen analyses,

$[PDDACl]_{0.24}[PDDA]_{0.29}V_2O_5$, 0.29 mol of $PDDA^+$ is counterbalancing V^{4+} in the compound that has two vanadium atoms. This corresponds to 13% of total vanadium in the formula, which means that in this compound, the negative sites correspond to 13% of total vanadium, in a very good agreement with the results found by XPS spectroscopy (15% of V^{4+} ions in total vanadium).

In the $[PAHCl]_{0.28}[PAH]_{0.47}V_2O_5$ hybrid, the concentration of V^{4+} ions calculated by XPS was 21%, while the values found by elemental analyses and Mohr's method, that is, PAH^+ interacting with oxygen bound to V^{4+} ions, were of 23%, again in a very good agreement. Therefore, these results clearly indicate that the surface composition observed is representative of the bulk samples since the results obtained by a surface analysis, XPS, are in good agreement with bulk analyses of the elements present (CHN analyses and Mohr's method). They also indicate that the reduction of vanadium ions is essential to the intercalation of polyelectrolytes, suggesting that no extra reduction agent is needed in this process.

It was shown previously [33] that PDDACl intercalation is very sensitive to the temperature and time of reaction: the increase in temperature of hydrothermal treatment increases the V^{4+}/V^{5+} ratio until in reactions at 180 °C, a new phase containing only V^{4+} ions is produced (VO_2) by oxidation of polyelectrolyte. Therefore, the conditions used in the present study afford the V^{4+}/V^{5+} ratio observed with very high reproducibility and forming a mixed valence vanadium oxide that presents intercalated PDDACl or PAHCl polycations.

3.4. Study of cyanine dye intercalation into the interlayer space of $[PDDACl]_{0.24}[PDDA]_{0.29}V_2O_5$

The intercalation of the anionic cyanine dye was performed in order to check on the real capacity for anion exchange in these materials. X-ray diffraction shows that after the encapsulation of the cyanine dye molecule into $[PDDACl]_{0.24}[PDDA]_{0.29}V_2O_5$ (Fig. 11), the interlayer spacing does not change significantly. It is possible that the basal space of $[PDDACl]_{0.24}[PDDA]_{0.29}V_2O_5$ hybrid material is enough to accommodate the cyanine guest molecules inside it without significant disturbance in the material (see size of dye molecule in Fig. 2). The same calculations showed that the most stable cyanine configuration is the planar one.

The results of CHN elemental analysis for $[PDDACl]_{0.24}[PDDA]_{0.29}V_2O_5$ (Table 1) were compared to $[PDDACy]_{0.08}[PDDACl]_{0.16}[PDDA]_{0.29}V_2O_5$ hybrid material and related to the difference between the quantities of carbon before and after cyanine intercalation reaction. This comparison indicated that a weight loss of approximately 6.20% could be expected in TGA after cyanine adsorption, and it was indeed observed (Supplementary information).

In the FTIR spectrum of $[PDDACy]_{0.08}[PDDACl]_{0.16}[PDDA]_{0.29}V_2O_5$ hybrid material, a new band appeared at 1191 cm^{-1} attributed to the antisymmetric stretching vibration of sulfonate groups in the cyanine dye (see Supplementary material, Fig. S1) [21]. Thus, these observations suggest the coexistence of polycations and cyanine dye within the interlayer space of the matrix. This is in agreement with the XRD measurement, suggesting a loops and tails configuration of the PDDACl chains in hybrid material as already commented by Hata et al. [22].

In the UV–Vis absorption spectrum of the *bulk* cyanine dye in methanol solution (Fig. 12a), a band around 552 nm is observed and indicates the absorbance of the monomer (broad band) with a hypsochromic shoulder at 519 nm, typical of cyanine dyes [33]. Beside the absorption of the solid at 200–500 nm, the UV–Vis spectrum of $[PDDACy]_{0.08}[PDDACl]_{0.16}[PDDA]_{0.29}V_2O_5$ material (Fig. 12b) shows cyanine band at 586 nm with hypsochromic shoulder at 552 nm, which is red-shifted in relation to the absorption of pure cyanine. This band is associated with the absorption of chromophore groups present in cyanine dye, and its position depends on the

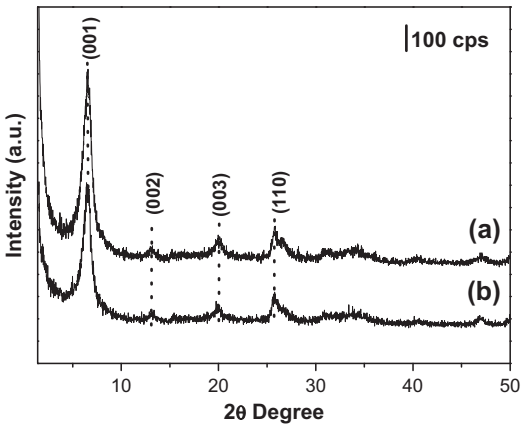

Fig. 11. Powder X-ray diffraction of $[PDDACl]_{0.24}[PDDA]_{0.29}V_2O_5$ hybrid (a) and $[PDDACy]_{0.08}[PDDACl]_{0.16}[PDDA]_{0.29}V_2O_5$ hybrid material (b).

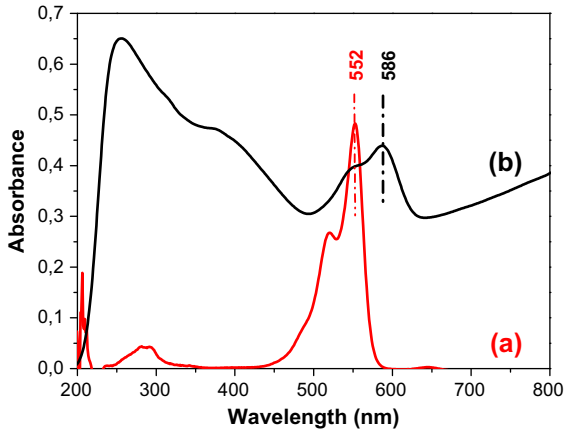

Fig. 12. UV–Vis spectrum of cyanine dye (8.56 μmol L^{-1} in methanol) (a) and UV–Vis diffuse reflectance spectrum of $[PDDACy]_{0.08}[PDDACl]_{0.16}[PDDA]_{0.29}V_2O_5$ hybrid material (b).

aggregation and adsorption state of dyes on the internal or external surfaces of the host materials [34,35]. The large red-shift (34 nm) can be due to the formation of J-type aggregates of anionic cyanine dye on the hybrid material [34,35].

The photoluminescence of hybrid material exchanged with cyanine dye was also examined. Fig. 13 shows the main fluorescence findings for the hybrid $[PDDACy]_{0.08}[PDDACl]_{0.16}[PDDA]_{0.29}V_2O_5$ and for the cyanine dye in methanol solution.

The emission spectrum of the cyanine dye solution shows one strong emission band at 598 nm when the dye is excited at 560 nm (Fig. 13a). When the hybrid material was excited at the same wavelength, a maximum emission band at 617 nm was observed (Fig. 13b). This red-shift relative to the emission band of cyanine dye in methanol should be due to the formation of aggregates, in agreement with DR UV–Vis study (Fig. 12), and to environmental polarity factors. It is well-known that the photophysical behavior of trapped molecules in inorganic matrices depends on several parameters, and for the intercalated system examined here, the spatial constriction caused by confinement due to layers may result in motional restriction for the excited cyanine guest molecules, which would trigger fast internal conversion relaxation processes [36]. Besides that, polarity in the interlayer space can dramatically affect optical properties of a confined dye, and an increase in polarity often leads to the formation of a red-shifted excited state [36,37]. In this case, the layered space of hybrid materials has a more pronounced polarity compared to the methanol, because there are PDDACl and

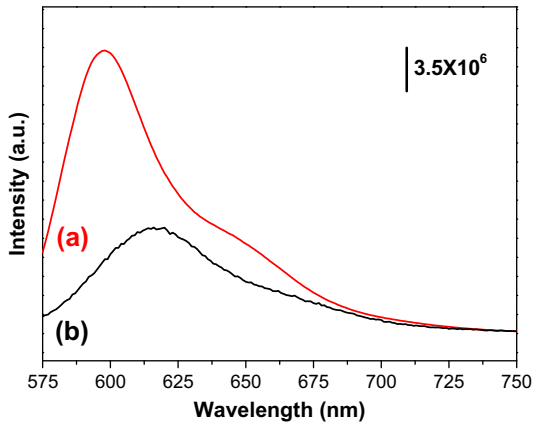

Fig. 13. Emission spectra at room temperature (excitation wavelength of 560 nm) of cyanine dye in (a) methanol solution (5×10^{-5} mol L^{-1}) and (b) intercalated in $[PDDACy]_{0.08}[PDDACl]_{0.16}[PDDA]_{0.29}V_2O_5$ hybrid material.

water molecules in the hybrid material (see Supplementary material, Fig. S2); therefore, the red-shift will be larger when the cyanine dye is confined in this solid matrix. Similar DR UV–Vis and photoluminescence results were obtained for cyanine intercalated in $[PAHCl]_{0.28}[PAH]_{0.47}V_2O_5$ hybrid material.

Similar studies are underway using PDDACl and PAHCl polyelectrolytes and cyanine dye in molybdenum oxide (MoO_3). These results will be reported in a future publication.

4. Conclusions

The present study describes a novel direct method of intercalation of cationic polyelectrolytes into *bulk* vanadium pentoxide, through the use of a hydrothermal treatment. Such experimental conditions caused a partial reduction of V^{5+} to V^{4+} centers of the oxide sheets and allowed the intercalation of PDDACl and PAHCl polyelectrolytes as charge balancing entity. The results obtained suggest that the polyelectrolyte intercalated in a fashion such that R_3N^+–Cl^- and NH_3^+—Cl^- ion pairs remain available, because Cl^- ions could be exchanged with nitrate ions and precipitated by silver. By using the obtained $[PDDACl]_{0.24}[PDDA]_{0.29}V_2O_5$ and $[PAHCl]_{0.28}[PAH]_{0.47}V_2O_5$ hybrids as the starting materials, and taking advantage of chloride exchange sites, novel vanadium pentoxide–anionic dye composites were synthesized. The lamellar structure of V_2O_5 is stable under these experimental procedures and is still found in the compounds obtained. UV–Vis and photoluminescence spectroscopy showed that the cyanine dye-based hybrid materials absorb in the visible region and has an emission peak at 617 nm. Because of their optical properties, these novel materials may be used in energy-storage, solar energy conversion and electronic devices. This study was focused in the preparation of novel lamellar anionic exchangeable hybrid materials, and their properties were assessed through the intercalation of a luminescent dye. It is of note that there are many other possible uses of these hybrid materials, for example, the adsorption of environmental contaminants such as $Cr_2O_7^{2-}$ and ClO_4^- or even of relevant biomolecules such as DNA.

Acknowledgments

The authors acknowledge the Fundação de Amparo à Pesquisa no Estado de São Paulo (FAPESP), the Piedmont Region (Italy) [NANOLED project (Novel Nanostructured Materials for Light Emitting Devices and Application to Automotive Displays), CIPE 2006] and the European Community [INNOVASOL project (Innovative Materials for Future Generation Excitonic Solar Cells), of the FP7] for the financial support to this work and to Conselho Nacional de Desenvolvimento Científico e Tecnológico (CNPq) for the fellowships. Dr. Caterina Benzi from University of Turin is gratefully acknowledged for the calculation of the dimensions of cyanine Iris 3.5b dye.

Appendix A. Supplementary material

Supplementary data associated with this article can be found, in the online version, at doi:10.1016/j.jcis.2011.11.013.

References

[1] M. Petras, B. Wichterlova, J. Phys. Chem. 96 (1992) 1805–1809.
[2] E. Shouji, D.A. Buttry, Langmuir 15 (1999) 669–673.
[3] M. Darder, M. Colilla, E. Ruiz-Hitzky, Appl. Clay Sci. 28 (2005) 199–208.
[4] T.A. Kerr, H. Wu, L.F. Nazar, Chem. Mater. 8 (1996) 2005–2015.
[5] C.V.S. Reddy, A.P. Jin, X. Han, Q.Y. Zhu, L.Q. Mai, W. Chen, Eletrochem. Commun. 8 (2006) 279–283.
[6] M.A. Gimenes, L.P.R. Profeti, T.A.F. Lassali, C.F.O. Graeff, H.P. Oliveira, Langmuir 17 (2001) 1975–1982.
[7] A.A. Teixeira-Neto, L. Marchese, G. Landi, L. Lisi, H.O. Pastore, Catal. Today 133 (2008) 1–6.
[8] M. Darder, M. Lopez-Blanco, P. Aranda, F. Leroux, E. Ruiz-Hitzky, Chem. Mater. 17 (2005) 1969–1977.
[9] D. O'Hare, in: D.W. Bruce, D. O'Hare (Eds.), Inorganic Materials, John Wiley and Sons, 1992, p. 254.
[10] D.W. Murphy, P.A. Christian, F.J. Disalvo, J.V. Waszczak, Inorg. Chem. 18 (1979) 2800–2803.
[11] M. Iwamoto, H. Furukawa, K. Matsukami, T. Takenaka, S. Kagawa, J. Am. Chem. Soc. 105 (1983) 3719–3720.
[12] Y.P. Zhang, C.J. OConnor, A. Clearfield, R.C. Haushalter, Chem. Mater. 8 (1996) 595–597.
[13] Y.K. Shan, R.H. Huang, S.P.D. Huang, Angew. Chem. Int. Ed. 38 (1999) 1751–1754.
[14] D. Riou, G. Ferey, J. Solid State Chem. 120 (1995) 137–145.
[15] T. Chirayil, P.Y. Zavalij, M.S. Whittingham, Chem. Mater. 10 (1998) 2629–2640.
[16] A.V. Murugan, J. Power Sources 159 (2006) 312–318.
[17] A.V. Murugan, C.W. Kwon, G. Campet, B.B. Kale, A.B. Mandale, S.R. Sainker, C.S. Gopinath, K. Vijayamohanan, J. Phys. Chem. B 108 (2004) 10736–10742.
[18] Y. Wang, G.Z. Cao, Chem. Mater. 18 (2006) 2787–2804.
[19] (a) K. Ohtsuka, Chem. Mater. 9 (1997) 2039–2050;
(b) F. Cavani, F. Trifiro, A. Vaccari, Catal. Today 11 (1991) 173–301;
(c) J.M. Oh, T.T. Biswickm, J.H. Choy, J. Mater. Chem. 19 (2009) 2553–2563.
[20] G. Decher, Science 277 (1997) 1232–1237.
[21] L.V.A. Gurgel, J.C.P. de Melo, J.C. de Lena, L.F. Gil, Bioresour. Technol. 100 (2009) 3214–3220.
[22] H. Hata, Y. Kobayashi, T.E. Mallouk, Chem. Mater. 19 (2007) 79–87.
[23] R.N. Smith, M. McCormick, C.J. Barrett, L. Reven, H.W. Spiess, Macromolecules 37 (2004) 4830–4838.
[24] A. Dorris, S. Rucareanu, L. Reven, C.J. Barret, R.B. Lennox, Langmuir 24 (2008) 2532–2538.
[25] F. Sediri, N. Gharbi, J. Phys. Chem. Solids 68 (2007) 1821–1829.
[26] V.V. Formichev, P.I. Ukrainskaya, T.M. Ilyin, Spectrochim. Acta Part A 53 (1997) 1833–1837.
[27] A.G. Souza, O.P. Ferreira, E.J.G. Santos, J. Mendes, O.L. Alves, Nano Lett. 4 (2004) 2099–2104.
[28] S. Pavasupree, Y. Suzuki, A. Kitiyanan, S. Pivsa-Art, S. Yoshikawa, J. Solid State Chem. 178 (2005) 2152–2158.
[29] C.W. Kwon, A.V. Murugan, G. Campet, J. Portier, B.B. Kale, K. Vijaymohanam, J.H. Choy, Electrochem. Commun. 4 (2002) 384–387.
[30] K.Q. Lai, A.G. Kong, F. Yang, B. Chen, H.M. Ding, Y.K. Shan, S.P. Huang, Inorg. Chim. Acta 359 (2006) 1050–1054.
[31] Y.J. Liu, J.L. Schindler, D.C. DeGroot, C.R. Kannewurf, W. Hirpo, M.G. Kanatzidis, Chem. Mater. 8 (1996) 525–534.
[32] F.J. Anaissi, G.J.F. Demets, R.A. Timm, H.E. Toma, Mater. Sci. Eng. A 347 (2003) 374–381.
[33] F.J. Quites, H.O. Pastore, Mater. Res. Bull. 45 (2010) 892–896.
[34] N. Miyamoto, R. Kawai, K. Kuroda, M. Ogawa, Appl. Clay Sci. 16 (2000) 161–170.
[35] (a) M. Ogawa, Chem. Mater. 8 (1996) 1347–1349;
(b) L. Latterini, M. Nocchetti, G.G. Aloisi, U. Costantino, F. Elisei, Inorg. Chim. Acta 360 (2007) 728–740.
[36] W. Xu, D.L. Akins, J. Phys. Chem. B 106 (2002) 1991–1994.
[37] H.Q. Guo, X.M. Zhang, M. Aydin, W. Xu, H.R. Zhu, D.L. Akins, J. Mol. Struct. 689 (2004) 153–158.